WOOD RESEARCH
63 (1): 2018
25-34

NANO-Fe_3O_4/ NMMO-CELLULOSE COMPOSITE MEMBRANE PREPARED BY THE IN-SITU CO-PRECIPITATION METHOD

Xiaojun Ma
Tianjin University of Science & Technology
College of Packaging & Printing Engineering Department of Wood Science and Technology
Tianjin, China

Xiaojun Zhang
Tianjin Food Safety & Low Carbon Manufacturing Collaborative Innovation Centertianjin, China

(Received December 2017)

ABSTARCT

Using NMMO-cellulose membrane as a matrix, Fe_3O_4/ cellulose composite membrane were prepared by the in-situ co-precipitation method. The effects of Fe^{2+} and Fe^{3+} salts concentration on the structure and properties of composite membranes were studied by scanning electron microscopy(SEM), X-ray diffraction(XRD), Fourier transform infrared spectrometer(FTIR) and vibrating sample magnetometer(VSM). Results showed that the spherical magnetic Fe_3O_4 nanoparticleswere dispersed uniformly and immobilized in the cellulose membranes, and there were good interactions between cellulose and Fe_3O_4 in the membranes. With increased iron ion content, the thermal stability of Fe_3O_4-CMgradually increases, and the complex membrane has a second significant weightlessness peak within 620–700 °C. In addition, it is also found that Fe_3O_4/cellulose composite membranes showed good superparamagnetic property.

INTRODUCTION

Magnetic membrane materials have not only the characteristics of magnetic recording, magnetic separation and magnetic absorption, but also the advantages of macromolecular materials, such as light weight, good chemical stability, excellent machinability and so on (Hajji et al. 1996, Ciardelliet al. 2001). In the present, magnetic membrane materials are applied for medical, aerospace, separation, electromagnetic shielding, stealth materials, and so on (Zhi et al. 2006, Calvo et al. 2012, Maleki et al. 2014, Qin et al. 2015). With the shortage of fossil resources and increasing of environmental awareness, more and more attentions are focused on the research

of natural-based matrix replacing of the traditional plastic-based matrix of Magnetic membrane materials.

Cellulose, the most abundant natural polysaccharide in the world, possesses unique properties such as nontoxicity, recyclability, and low cost. However, cellulose is difficult to prepare membrane materials because of its insolubility, which results from the strong hydrogen bonding between intra-molecular and inter-molecular. Therefore, some solvent systems have been reported to solve the problem, for example, NMMO, LiOH/urea/water, LiCl/N, N-dimethylacetamide, and so on (Kuga et al. 1980, Mccormick et al. 1985, Swatloski et al. 2002, Cai et al. 2005,Mao et al. 2006, Liet al. 2010).At the same time, as a result of the cellulose has a lot of nanoscale aperture, which provides a good template for the deposition and load of the magnetic nano materials.

Superparamagnetic particle materials include Ni, Co, Fe, Fe_2O_3,Fe_3O_4, Fe–Co, and Ni–Fe (Kluchova et al. 2009, Liu et al. 2011). Among these, Magnetite (Fe_3O_4) nanoparticle has attracted significant attention in recent years not only because of its unique size and morphology dependent physical and chemical properties, but also for its biocompatibility and remarkable magnetic properties (Chiscan et al. 2012, Maleki et al. 2014). Therefore, it is expected that the spherical Fe_3O_4/cellulose membrane materials can be designed and biosynthesized.

In the present work, cellulose were dissolved in aqueous (N-methylmorpholine N-oxide) NMMO solution to prepare membranes as matrices. Next, nano-Fe_3O_4/ NMMO-cellulose membrane were synthesized by the in-situ co-precipitation method. The effects of Fe^{2+} and Fe^{3+} salts concentration on the structure and properties of composite membranes were studied by scanning electron microscopy(SEM), X-ray diffraction(XRD), Fourier transform infrared spectrometer(FTIR) and vibrating sample magnetometer(VSM). The information gained in this study could be useful for designing low-cost, easily available adsorbents based on cellulose and further practical applications in color removal from dye-containing effluents.

MATERIALS AND METHODS

Materials

Hardwood pulp paddleswere provided from Shandong Hailong Co. Ltd (Shanghai, China). N-methylmorpholine N-oxide (NMMO, 50%) and propyl gallate (PG, 98%) wassupplied by Shanghai Ginchun Chemicals Reagent Co. Ltd (Shanghai, China). Ferrous chloride tetrahydrate($FeCl_2$•$4H_2O$, hexahydrate ferric chloride ($FeCl_3$•$6H_2O$) and sodium hydroxide (NaOH) were purchased from Tianjin Jiangtian Chemical Reagent Company (Tianjin, China). Other reagents were analytically pureand used without further purification. Ultrapure water was used throughout the experiment.

Preparation of NMMO-cellulose membranes (CM)

Propyl gallate (0.5 wt.%) as an antioxidant was added in aqueous (N-methylmorpholine N-oxide)NMMO solution which was distilled until the surplus water decreasing to 13.3 wt.% under ultrasonic agitation at 95°C for 30 min, then the dried hardwood pulp paddles (5.0 wt.%) were added into this beaker at 98°C for 4.5 h with static. The dissolved cellulose was stirred at 98°C for 4.5 h to form homogeneous and transparent cellulose/NMMO/H_2O solution, and the above mixture was poured and casted with a copper string onto the glass to obtain cellulose membranes.

Preparation of Fe_3O_4/NMMO-Cellulose composite membranes (Fe_3O_4-CM)

Fe_3O_4/ cellulose membranes were prepared by the in-situ co-precipitation method. The obtained membranes were immersed in a 200mL mixture of aqueous $FeCl_3 \cdot 6H_2O$ and $FeCl_2 \cdot 4H_2O$ (1.8:1 of molar ratio) for 12 h.Then, the composite was put into 200mL of aqueous NaOH (0.2 mol/L) for 40 min under N_2 gas to prevent oxidation. After that, the composite was washed with distilled water until the pH reached 7. Finally, the resulting product was dried at 60 °C for 4 h to obtain Fe_3O_4/cellulose composite membranes. The relevant chemical reaction can be expressedas follows:

$$Fe^{2+} + 2Fe^{3+} + 80H^- \rightarrow Fe_30_4 + 4H_20 \quad (1)$$

Tab. 1 was Iron ion concentration in different Fe_3O_4/ cellulose membranes. The concentrations of Fe^{2+} and Fe^{3+} in the sample were calculated with the molar mass of the reaction solution.

Tab. 1: Iron ion concentration in different samples.

Iron ion (mol•L^{-1})	a	b	c	d	e
Fe^{2+}	0.150	0.190	0.230	0.270	0.310
Fe^{3+}	0.190	0.342	0.414	0.486	0.558

Characterization

Wide-angle X-ray diffraction (XRD) measurements were carried out on an XRD diffractometer (D/max2500, Rigaku, USA). Morphology of chemical cured fibers were observed by scanning electronic microscopy (FESEM; S-800, Hitachi, Japan) using gold-coated samples at an accelerating voltage of 10 kV.Fourier transform infrared (FT-IR) spectroscopy was carried out on an FT-IR spectrophotometer (Nicolet 6700, Bruker, USA), using the KBr disk method. The weight loss behaviors and decomposition temperature (T_d) of samples were measured by using thermogravimetric analysis (TGA) on a simultaneous thermal analyzer (TG-209, Netzsch, Germany) from room temperature to 1000°C with the heating rate of 30°C·min^{-1} in high pure nitrogen stream (30 ml·min^{-1}).A vibrating sample magnetometer (Lakeshore, 7304, USA)was used to measure the magnetic properties of the composite at room temperature.

RESULTS AND DISCUSSION

XRD analysis

Fig. 1 shows the X-ray diffraction patterns of the samples. The 2θ data of all samples have (110), (110) and (200) characteristic peaks of cellulose at 12.5˚,20.5˚ and 35.2˚, respectively. This result indicates that the complex of Fe_3O_4 nanoparticles on the cellulose membrane, through the in situ chemical co-precipitation process, does not destroy the molecular and fiber structures of the membrane.The diffraction intensity of the three characteristic peaks of the cellulose in the samples decreased with the increase of iron ion concentration. This phenomenon demonstrates that the in situ complex has altered the degree of crystallinity of cellulose in the magnetic cellulose membrane. All X-ray diffraction patterns of the complex membrane show diffracted peaks near 2θ = 30.3˚, 35.7˚,43.4˚,57˚ and 63.3˚, which correspond to the (220) ,(400),(422),(511) and (440) crystal surface of Fe_3O_4. This result is basically consistent with the characteristic peak of inverse spinel Fe_3O_4. Thus, Fe_3O_4 nanoparticles are successfully loaded on the surface of cellulose membrane through chemical co-precipitation method.

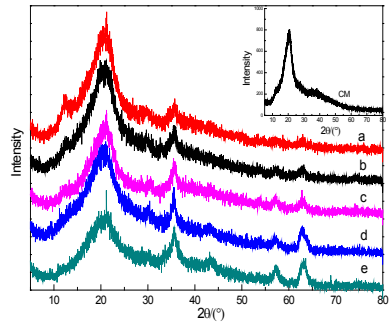

Fig. 1: XRD pattern of Fe_3O_4/ cellulose composite memberane materials.

With increased iron ion content, the width and intensity of Fe_3O_4 characteristic peak continuously increase. Increasing the iron ion content improves the degree of crystallinity of the nano-Fe_3O_4, thereby enlarging thegrainsize.

Tab. 2: Average particle size of Fe_3O_4 nanoparticles preparing by different concentration of iron ion.

Samples	a	b	c	d	e
2θ/°	35.64	35.68	35.78	35.74	35.78
The average particle size (nm)	17.6	18.5	21.4	20.6	26.5

Scherrer formula is used to calculate the original average grain size of the magnetic nanoparticles in the complex membrane, and this value is found to be 21 nm (Tab. 2). The average grain size of the Fe_3O_4 nanoparticles gradually increases when the concentration of iron ion increases. The increase in average grain size enhances the degree of crystallinity of the complex membrane, thereby improving mechanical performance (Zhou et al. 2009). The increasing grain size accelerates the motion of the electrons and augments the conductive properties of the membrane.

SEM analysis

Fig. 2 shows the SEM micrographs of the different samples. Compared with treated samples, the surface morphology of the original cellulose membrane is smoother, with sponge-like porous structure (Fig. 2a). This characteristic facilitates the deposition of the Fe_3O_4 nanoparticles on the surface membrane. Most Fe_3O_4 nanoparticles generated on the cellulose membrane are globular (Fig. 2b). Fe_3O_4 nanoparticles are embedded uniformly in the cellulose matrix, without clustering. However, Fe_3O_4 nanoparticles clusters significantly in Fig. 2d, with different grain sizes. This phenomenon indicates that the excessive increase in the iron content results in a remarkable cluster generated of nanoparticles Fe_3O_4. The surface morphology of the complex materials shows that the Fe_3O_4 nanoparticles are embedded in the surface of the cellulose substrate and closely combined with cellulose via electrostatic attraction and van der Waals force.

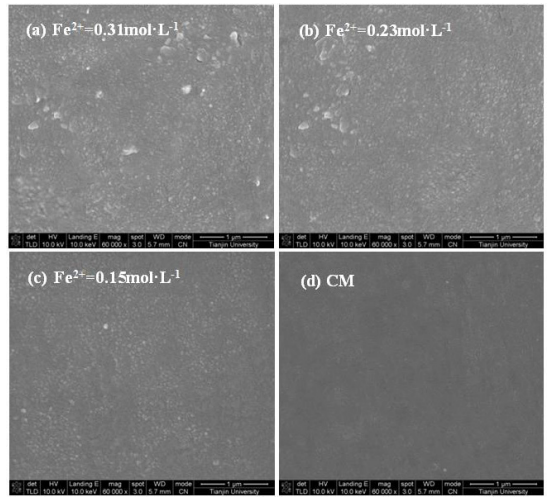

Fig. 2: SEM photographs of different samples.

FTIR analysis

Fig. 3 shows the FTIR spectra of the cellulose and complex membranes. The absorption peaks at 3420 and 1640 cm^{-1} correspond to the stretching and bending vibrations of O-H, which are due to the -OH vibration of cellulose in the complex. The absorption peak near 2900 cm^{-1} is attributed to the C-H stretching vibration of cellulose in the complex. The absorption peaks at 1061 and 895 cm^{-1} that correspondsto the C-O and C-C stretching vibrations prove the existence of cellulose in the complex. A Fe-O vibration absorption peak at 594 cm^{-1} is also observed, and this peak proves the existence of Fe_3O_4 in the complex (Zhou et al. 2009). With increased iron ion content, the absorption peak at this point is enhanced significantly.In addition, the hydroxyl characteristic peaks at 3420, 2900, and 1640 cm^{-1} are significantly weakened, and they move to low-wave regions. This phenomenon suggests that the magnetic particles not only form hydrogen bonds by combining with the cellulose surface, but also produce chemical bonds with hydroxyl on the cellulose surface to reduce hydroxyl. Thus, chemical bonding and physical adsorption were found in the Fe_3O_4/cellulose complex membrane.

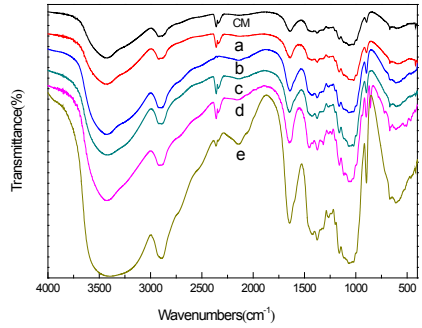

Fig. 3: FT-IR spectra of different samples.

Thermogravimetric analysis

Fig. 4 shows the TG and DTG curves of the cellulose and complex membranes. The samples were slightly loss of weight at the beginning of the temperature rise. Weight loss is over at 150°C because of the removal of the adsorbed water and residual organics from samples of the complex materials. The main weight loss occurs at 250–350°C. All samples exhibit remarkable weightloss peaks. The weight loss (approximately 47-63%) is mainly due to the thermal decomposition of the wooden cellulose (thermal decomposition temperature is in the range of 260-340°C). Moreover, at this stage, the weight loss of the cellulose membrane is obviously higher than that of the complex membrane. Additionally, the thermal decomposition temperatures of all complex membranes are higher than those of the cellulose membrane. This characteristic signifies that the interface adhesion between the Fe_3O_4 nanoparticles and cellulose membrane improves the thermal stability of the complex membrane. The DTG diagram of the samples demonstrates that the maximum decomposition temperature for the complex membrane is not gradually improved with increased iron ion content. This behavior may have been caused by the intense clustering of the nanoparticles with the increase in load, and the decreased interface adhesion reduces the thermal decomposition temperature.

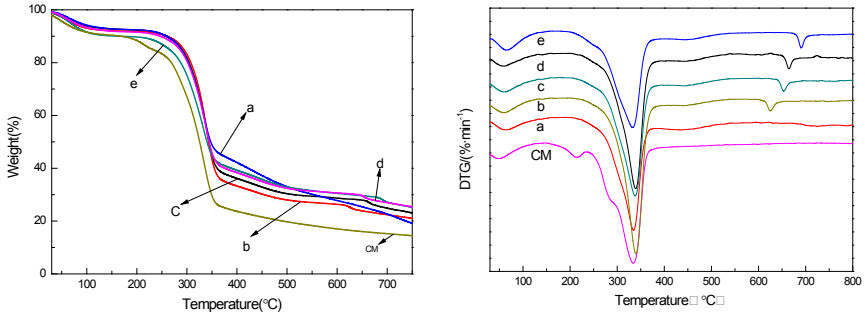

Fig.4: TG and DTG curves of different samples.

After the temperature was raised to 350°C, the thermal weight loss of the cellulose membrane levels off, which is mainly due to the complete decomposition of the cellulose produced a small amount of coke, furfural and other substances to continue degradation. In addition, the complex membrane has a second significant weightloss peak within 620–700°C. Within this temperature range, the cellulose has been decomposed completely. The decomposition temperature for the Fe_3O_4 nanoparticles (1538°C) is considerably higher than the temperature interval for the second weightloss of the complex membrane. Therefore, within 620–700°C, the cellulose–Fe_3O_4 complex, with the combined effects of Fe_3O_4 nanoparticles in the compound materials, can be decomposed. Moreover, with increased iron ion content, the second weightloss peak in the complex membrane moves to a higher temperature, and weightloss temperature significantly increases. This behavior indicates that the increase in iron ion content improves the binding force between the cellulose and Fe_3O_4 nanoparticles, and this phenomenon is beneficial for enhancing the thermal stability of the complex membrane (Tab. 3).

The residual amount of the complex membrane (27.18%) is remarkably higher than that of the cellulose membrane (13.45%). With increased iron ion content, the composite volume of the Fe_3O_4 nanoparticles on the cellulose membrane is also improved. Moreover, the TG diagram shows that the thermal weightloss curve of the complex membrane is smoother than that of the cellulose membrane. Thus, Fe_3O_4 nanoparticles are embedded on the surface of the

Tab. 3: The temperature of maximum weight loss rate of different samples.

Samples	CM	a	b	c	d	e
The maximum temperature of the first weight loss(°C)	329.21	334.71	337.73	339.24	340.77	334.88
The maximum temperature of the second weight loss(°C)	-	-	624.52	653.31	664.27	691.13
Residual weight ratio(%)	13.45	22.45	22.32	23.66	27.11	27.18

cellulose membrane or filled in the matrix via chemical co-precipitation process. Both of these cases are closely combined by electrostatic attraction and van der Waals force. This characteristic effectively improves the thermal stability of cellulose complex membrane.

VSManalysis

Fig. 5 shows the magnetic hysteresis loops of the complex membrane. The magnetic hysteresis loops of Fe_3O_4-CM are basically coincident except 0.31 mol•L^{-1}. Remanent magnetization intensity approaches zero, with lower coercive force. This characteristic indicates that samples have better super-paramagnetic property at room temperature. However, when the Fe^{2+} content is increased to 0.31 mol•L^{-1}, the magnetic hysteresis loops of the samples are no longer coincident. Additionally, the coercive force and residual magnetization of the complex membrane are increased. This result indicates that with increased iron ion content, the Fe_3O_4 nanoparticles on the cellulose membrane cluster, causing the dimensions to be higher than the super-paramagnetic critical dimension of the membrane. Magnetic nanoparticles have higher coercive force, causing samples to lose their super-paramagnetism (Zhu et al. 2011, Zhao et al. 2016).

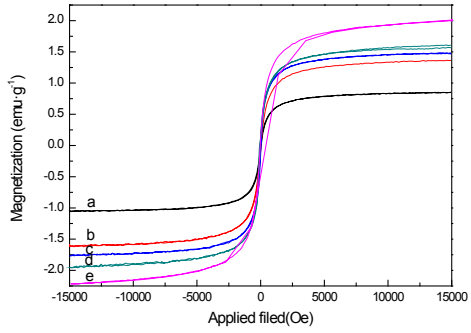

Fig.5: Magnetic hysteresis loop of cellulose composite materials

Tab. 4: The remanent magnetization ,coercivity and saturation magnetization of cellulose composite materials.

Samples	a	b	c	d	e
Remanent magnetization(emu/g)	0.043	0.064	0.087	0.172	0.451
Coercivity(A/m)	21.4	22.5	22.7	42	335
Saturation magnetization(emu/g)	0.85	1.36	1.47	1.59	2.01

Tab. 4 shows that, with increased iron ion content, remanent magnetization intensity, coercive force, and saturation magnetization of samples significantly increase. This phenomenon indicates that the increase of iron ion content has a great influence on the the saturation magnetization of the complex membrane. Increasing the iron ion content intensifies the clustering of the Fe_3O_4 nanoparticles, resulting in strong crystallinity and larger grain size. Therefore, the saturation magnetization intensity is higher than that of the complex membrane with smaller grain size.

CONCLUSIONS

Fe_3O_4-CM are prepared by the in-situ co-precipitation method and using NMMO-cellulose membrane as a matrix. The spherical magnetic Fe_3O_4 nanoparticles are dispersed uniformly and immobilized in the cellulose membranes, and there are good interactions between cellulose and Fe_3O_4 in the membranes. With increased iron ion content, the thermal stability of Fe_3O_4-CM gradually increases. It is also found that Fe_3O_4/cellulose composite membranes shows good superparamagnetic property.

ACKNOWLEDGMENTS

This research was financially supported by National Natural Science Foundation of PR China (No. 31270607).

REFERENCES

1. Cai, J., Zhang, L., 2005: Rapid dissolution of cellulose in LiOH/urea and NaOH/urea aqueous solutions, Macromolecular Bioscience 5(6): 539–548.
2. Calvo, S., Arias, N. P., Giraldo, O., Rosales-Rivera, A.,Moscoso, O., 2012: Thermal and magnetic behavior of angustifolia kunth bamboo fibers covered with Fe_3O_4 particles, Physica B Condensed Matter407(16): 3267-3270.
3. Ciardelli,G., Corsi, L., Marcucci, M., 2001: Membrane separation for wastewater reuse in the textile industry, Resources Conservation & Recycling 31(2): 189-197.
4. Chiscan, O., Dumitru, I., Postolache, P., Tura, V., Stancu, A., 2012: Electrospun PVC/Fe_3O_4 composite nanofibers for microwave absorption application, Materials Letters 68(2): 251-254.
5. Hajji, P., Cavaillé, J. Y., Favier, V., Gauthier, C., Vigier, G.,1996: Tensile behavior of nanocomposites from latex and cellulose whiskers. Polymer Composites 17(4): 612–619.
6. Kuga, S. 1980: The porous structure of cellulose gel regenerated from calcium thiocyanate solution, Journal of Colloid & Interface Science 77(2): 413-417.
7. Li, R., Chang, C., Zhou, J., Zhang, L., Gu, W., Li, C.,Liu,S.,Kuga,S.,2010: Primarily industrialized trial of novel fibers spun from cellulose dope in naoh/urea aqueous solution, Industrial & Engineering Chemistry Research 49(22): 11380-11384.
8. Liu, S., Zhou, J., Zhang, L., 2011: In situ synthesis of plate-like Fe_2O_3 nanoparticles in porous cellulose films with obvious magnetic anisotropy, Cellulose 18(3):1-11.

9. Kluchova, K., Zboril, R., Tucek, J., Pecova, M., Zajoncova, L., Safarik, I., Mashlan, M., Markova, I., Jancik, D. and Sebela, M., 2009: Superparamagnetic maghemite nanoparticles from solid-state synthesis—their functionalization towards peroral MRI contrast agent and magnetic carrier for trypsin immobilization, Biomaterials30(15):2855-2863.
10. Maleki, A., Ghamari, N., Kamalzare, M., 2014: Chitosan-supported Fe_3O_4, nanoparticles a magnetically recyclable heterogeneous nanocatalyst for the syntheses of multifunctional benzimidazoles and benzodiazepines, Cheminform 45(39): 9416-9423.
11. Maleki, A., Kamalzare, M., 2014: Fe_3O_4@cellulose composite nanocatalyst: Preparation, characterization and application in the synthesis of benzodiazepines, Catalysis Communications 53(30): 67-71.
12. Mao, Y., Zhou, J., Cai, J., Zhang, L.,2006:Effects of coagulants on porous structure of membranes prepared from cellulose in naoh/urea aqueous solution, Journal of Membrane Science279(1–2): 246-255.
13. Mccormick, C. L., Callais, P. A., Hutchinson, B. H., 1985: Solution studies of cellulose in lithium chloride and n,n-dimethylacetamide, Macromolecules 18(12): 2394-2401.
14. Qin,Y.,Qin,Z.,Liu,Y.,Cheng,M.,Qian,P.,Wang,Q.,Zhu,M.,2015:Superparamagnetic iron oxide coated on the surface of cellulose nanospheres for the rapid removal of textile dye under mild condition, Applied Surface Science 357: 2103–2111.
15. Swatloski, R. P., Spear, S. K., Holbrey, J. D., Rogers, R. D., 2002: Dissolution of cellulose with ionic liquids, American Chemical Society 124(18): 4974–4975.
16. Zhao, X., Li, H., Ding, A., Zhou, G., Sun, Y., Zhang, D., 2016: Preparing and characterizing Fe_3O_4 @cellulose nanocomposites for effective isolation of cellulose-decomposing microorganisms, Materials Letters 163: 154-157.
17. Zhi, J., Wang, Y., Lu, Y., Ma, J., Luo, G., 2006: In situ preparation of magnetic chitosan/Fe_3O_4 composite nanoparticles in tiny pools of water-in-oil microemulsion, Reactive & Functional Polymers 66(12): 1552-1558.
18. Zhou, J., Li, R., Liu, S., Li, Q., Zhang, L., Zhang, L., Guan, J., 2009: Structure and magnetic properties of regenerated cellulose/Fe_3O_4 nanocomposite films, Journal of Applied Polymer Science 111(5): 2477–2484.
19. Zhu, H., Jia, S., Wan, T., Jia, Y., Yang, H., Li, J.,Yan,L.,Zhong,C.,2011: Biosynthesis of spherical Fe_3O_4/bacterial cellulose nanocomposites as adsorbents for heavy metal ions, Carbohydrate Polymers 86(4): 1558-1564.

Xiaojun Ma*
Tianjin University of Science & Technology
College of Packaging & Printing Engineering
Department of Wood Science and Technology
Tianjin, 300222
China
Phone: +86-0-22-60274494
*Corresponding author: mxj75@tust.edu.cn

Xiaojun Zhang
Tianjin Food Safety & Low Carbon Manufacturing Collaborative Innovation
Centertianjin, 300457
China